INVITED PAPER *Special Section on Recent Progress in Antennas and Propagation in Conjunction with Main Topics of ISAP2016*

Arbitrarily-Shaped Reflectarray Resonant Elements for Dual-Polarization Use and Polarization Conversion

Hiroyuki DEGUCHI[†], ***Member***, **Daichi HIGASHI**[†a)], ***Student Member***, **Hiroki YAMADA**[†], **Shogo MATSUMOTO**, ***Nonmembers***, ***and*** **Mikio TSUJI**[†], ***Member***

SUMMARY This paper proposes a genetic algorithm (GA) based design method for arbitrarily-shaped resonant elements that offer enhanced reflectarray antenna performance. All elements have the specified phase property over the range of 360°, and also have dual-polarization and low cross-polarization properties for better reflectarray performance. In addition, the proposal is suitable for linear-to-circular polarization conversion elements. Thus, polarizer reflectarray elements are also presented in this paper. The proposed elements are validated using both numerical simulations and experiments.

key words: *reflectarray, infinite periodic array, dual-polarization, polarization conversion*

1. Introduction

Reflecarray antennas are very attractive as alternative to conventional parabolic reflector antennas because of their simple manufacturing process, low profile structure, lightness, and improved polarization performance [1]. It consists of a planar arrangement of resonant elements printed on a conductor-backed dielectric substrate. In recent, a reflectarray has been applied to a lot of application such as deployable reflector antennas [2], millimeter-wave imaging systems [3] and FSR (frequency selective reflector) to improve communication environment for blind area [4].

In the reflectarray antenna, phase distribution on its aperture is controlled by arranging resonant elements appropriately. Thus, it is possible to convert an incident wave front from an illuminator into reflection wave with desired wave-front. These phasing elements play an important role in determining the performance of the reflectarray antenna. In general, for developing reflectarray, the desirable resonant elements need to have the reflection phase property over the range of 360° at the specified frequency to control the aperture phase distribution, and also have low cross-polarization and dual-polarization. However, there is a major drawback that the reflectarray is usable only in narrow bandwidth because the reflection phase of each element greatly depends on the frequency. To improve the reflectarray performances, a lot of investigations have been so far reported in [5]–[10], and also have reported in [11]–[13] to suppressed cross-polarization. We have proposed multiple resonant elements such as dipole type ; convex-shaped elements [14], Ω-shaped elements [15], and four axial symmetric elements [16]. Furthermore, GA-optimized conductor elements have been reported in [17]–[20] to realize better performance. These proposed elements are usable only in linear polarization use. However, circularly polarized wave is often used in satellite communication systems so that polarizer-conversion is one of important techniques. Recently, some investigation for polarizer-conversion reflector [21]–[23] and thin lens [24] have been reported. However, it is difficult to keeping phase difference between two orthogonal polarizations. We also have applied the mechanism proposed in [24] to a reflectarray, and have already presented linear-to-circular polarizer reflectarray [25].

In this paper, we introduce configurations of the GA-optimized conductor resonant elements which have three kinds of a 90-degree rotational symmetric shape [17], a biaxial symmetric shape [18], and multiple-axial symmetric shape fulfilling both biaxial symmetry and 90-degree rotational symmetry [19], [20] for better performance of reflectarrays. Then, we proposes GA-optimization method to design polarizer-conversion elements [26] which have the phase difference of 90° between the TE and the TM waves with the desirable reflection phase range of 360°. To verify effectiveness of the proposed elements, a reflectarray is constructed by them and is evaluated by comparing of the radiation patterns between the calculated value and the measured one in the X-band.

2. Design Method

2.1 Analysis Method

Figure 1(a) shows a reflectarray with arbitrarily-shaped elements. Assuming an infinite periodic array, the reflection phase property for an oblique incident plane wave is analyzed by the method of moments (MoM) in spectral domain [27], [28]. The simultaneous linear equations in the MoM expanded by roof-top sub domain basis functions are solved by using FFT and are solved by the conjugate gradient method (CGM).

2.2 Optimization by GA and Design Condition

To design arbitrarily-shaped elements in Fig. 1, we use optimization technique using the genetic algorithm (GA). The

Manuscript received February 15, 2017.
Manuscript revised June 15, 2017.
Manuscript publicized August 22, 2017.

[†]The authors are with the Faculty of Science and Engineering, Doshisha University, Kyotanabe-shi, 610-0321 Japan.
a) E-mail: eup1302@mail4.doshisha.ac.jp

DOI: 10.1587/transcom.2017ISI0001

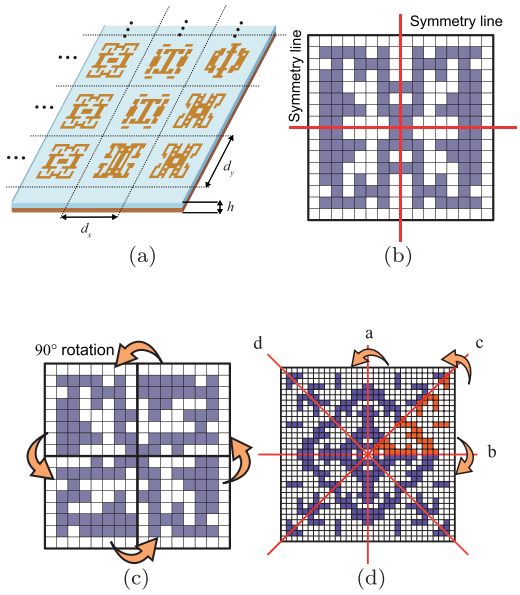

Fig. 1 Reflectarray structure and three kinds of geometry shapes.

conductor and no-conductor regions in the GA design are expressed it by "1" or "0", respectively. Symmetric configuration of the geometry shape as shown in Fig. 1(b) realize the element having low cross-polarization property. On the other hand, the 90-degree rotational symmetry shown in Fig. 1(c) realize the element having dual-polarization property. In the case of multiple-axial symmetry shown in Fig. 1(d), the element can have dual-polarization and low cross-polarization properties. Furthermore, the elements in Fig. 1(b) can be also used for designing linear-to-circular polarizer elements. These elements are designed by optimizing a quarter area or one-eighth of the unit-cell as an optimization variable in the GA.

We optimize the above reflecting-element shapes under the conditions of the oblique incident angle 30° at the center frequency 10.0 GHz. The dimension of the unit-cell in x and y directions are $d_x = d_y = 12.0$ [mm] to suppress the grating lobe in the specified frequency band (X-band). The thickness of dielectric substrate with permittivity $\epsilon_r = 1.67$ is $h = 3.0$ [mm], and the unit-cells shown in Fig. 1(b), (c) are divided into $N \times M = 16^2$ (0.75 mm/pix $\ll \lambda$) and Fig. 1(d) is divided into $N \times M = 32^2$ (0.375 mm/pix $\ll \lambda$) in order to apply roof-top basis function. One pixel in the unit cell is sufficiently smaller than the wavelength in the specified frequency band. We increase the division mesh in Fig. 1(d) to double as compared with that in Fig. 1(b) or (c) to raise the freedom of the element shape to be optimized. As GA parameters, we also set that generation number is 1000, population is 200, crossover value is 0.8, and mutation rate is 0.001. The average calculation time is 6 hours for each unit cell. The degradation of its gain keeps less than 0.35 dB in the case of the reflectarray elements having the phase of 30° interval [29]–[31]. We have parametrically simulated about the number of elements and tolerance α based on a point of the gain loss and calculation time in [29]–[31]. As a result, we use the number of elements $n = 12$ and tolerance $\alpha = 10°$ in this GA design.

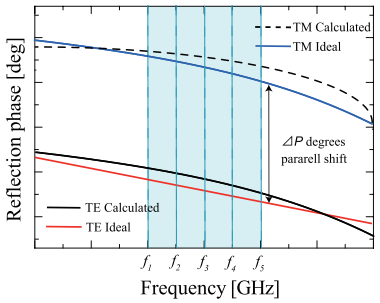

Fig. 2 Diagram of fitness function.

2.3 Evaluation Function

We apply the design method to the above-mentioned symmetric types. The evaluation function based on the reflection phases shown in Fig. 2 is as follows,

$$fitness = \sum_i F_{TE}(f_i) + \sum_i F_{TM}(f_i), \tag{1}$$

where

$$F_{\substack{TE\\TM}}(f_i) = w_{i_{\substack{TM}}^{TE}} |P_{\substack{TE\\TM}}(f_i) - P_{i_{\substack{TM}}^{TE}}|^2$$

$$w_{i_{\substack{TM}}^{TE}} = \begin{cases} 1 & (|P_{\substack{TE\\TM}}(f_i) - P_{i_{\substack{TM}}^{TE}}| > \alpha) \\ 0 & (|P_{\substack{TE\\TM}}(f_i) - P_{i_{\substack{TM}}^{TE}}| \le \alpha) \end{cases}$$

$$P_{iTM} = P_{iTE} + \Delta P.$$

$F_{TE}(f_i)$ and $F_{TM}(f_i)$ are evaluation parameters that are calculated at the i-th frequency point for the TE and the TM incidences, respectively. $w_{i_{\substack{TM}}^{TE}}$ is weighting factor. $P_{i_{\substack{TM}}^{TE}}$ is an ideal reflection-phase value, and also $P_{\substack{TE\\TM}}(f_i)$ is the calculated one at i-th frequency point. If difference of phases between the ideal value and the calculated one is less than tolerance α, $F_{\substack{TE\\TM}}(f_i)$ is set to zero. Otherwise, this value equal to the same value of phase difference. The ideal phase value is specified for the TE incidence, while ideal phase value for the TM incidence is automatically determined by adding desired phase-shift value ΔP. As the desired reflection-phase curves of the resonant elements for the TE incidence, we adopt here 12 linear functions with the slope of 60 [deg./GHz] for the frequency which are arranged every 30 degrees in parallel. Designing the elements under these conditions, we suppress deterioration of performance due to phase error. We have parametrically calculated the various slopes and determined the best slope of the phase-curve. If ΔP is 0° or 90°, the resulting elements have dual-polarization or linear-to-circular polarization property. The desirable element is obtained by minimizing its fitness value in the GA optimization. Although the convergence properties of generation depends on the elements, the proposed elements in this paper almost converge in less than 500 generations.

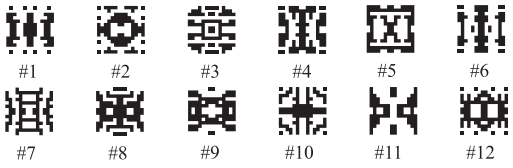

Fig. 3 Geometries with biaxial symmetric structure.

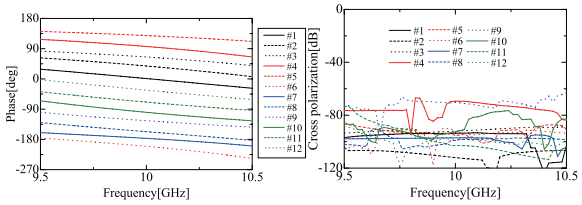

(a) Reflection phase. (b) Cross-polarization.

Fig. 4 Frequency responses of reflected wave for the oblique TE incidnce.

Fig. 5 Geometries with 90-degree rotational symmetric structure.

3. Comparison Between Three Types of Arbitrarily Shaped Reflectarray Elements

3.1 Single-Polarization Reflectarray Elements

Figure 3 shows the biaxial symmetric structures as optimized by GA. The frequency responses of the reflection phase of co-polarization and the amplitude properties of cross-polarization for the oblique TE incidence shown in Fig. 4(a) and (b), respectively. We can see from these figures that the phase shift is more than 360° over the specified frequency (9.5 GHz - 10.5 GHz) for the TE incidence, and also the amplitude properties of the cross-polarization level is suppressed to less than −60 dB. Because the current distribution on the element is axially symmetric, a pair of cross-polarized components directed in opposite directions are generated and the far fields of the cross polarized component cancel each other. It is clear from this example that the biaxial symmetric elements are useful for a single-polarization reflectarray with low cross-polarization.

3.2 Dual-Plarization Reflectarray Elements

Figure 5 shows the 90-degree rotationally symmetric structures. The frequency responses of the reflection phase of co-polarization for the oblique TE and the TM incidences shown in Fig. 6(a) and (b), respectively. The phase shift is more than 360° over the specified frequency; both incidences have virtually the same reflection phase properties. However, we can see that several phases (# 6 and # 7) are

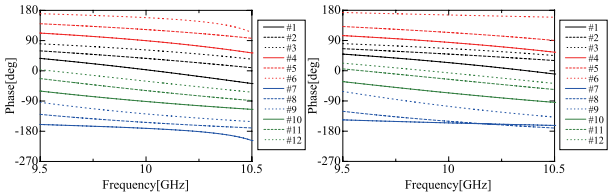

(a) TE incidence. (b) TM incidence.

Fig. 6 Frequency responses of reflection phase for the TE and the TM incidences.

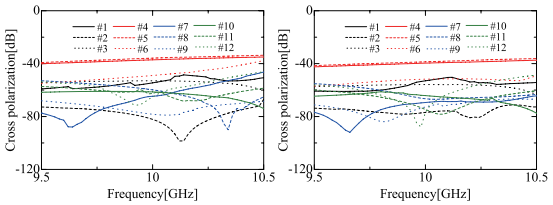

(a) TE incidence. (b) TM incidence.

Fig. 7 Amplitude properties of the cross-polarization for the TE and the TM incidences.

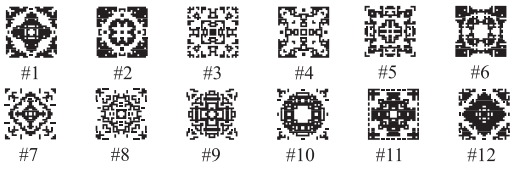

Fig. 8 Geometries with four-axial symmetric rotational symmetric structure.

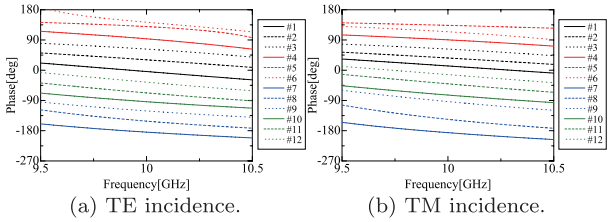

(a) TE incidence. (b) TM incidence.

Fig. 9 Frequency responses of reflection phase for the TE and the TM incidences.

not linear curve in near both ends of the specified frequency band because these elements do not fully converge. This phenomenon can be seen in the later figure (see # 6 and # 7 shown in Fig. 9 and # 5 and # 6 shown in Fig. 12). Although such elements a little deteriorate the performance, it is expected that the proposed elements works successfully by considering their appropriate arrangement on a reflectarray. Figure 7 plots the amplitude properties of cross polarization versus frequency. The cross-polarization level is suppressed less then about −40 dB by GA design. However, it is difficult to more suppress the cross polarization level in this symmetric type. Figure 8 shows the geometries with multiple-axial symmetric structure. These elements are biaxially symmetrical and 90-degree rotationally symmetrical. Figure 9 shows the reflection phase properties for the TE and the TM incidences. The reflection phase exhibit a set of almost linear

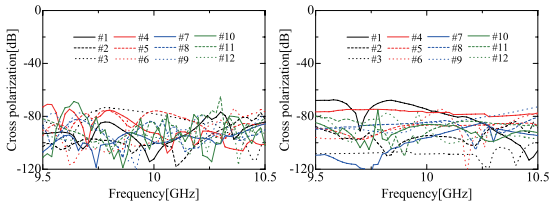

(a) TE incidence. (b) TM incidence.

Fig. 10 Amplitude properties of the cross-polarization for the TE and the TM incidences.

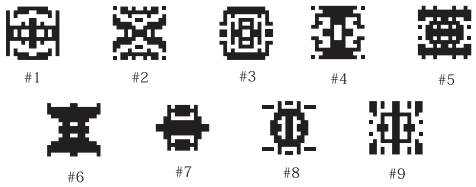

Fig. 11 Geometries for polarization conversion.

and parallel curves, and the reflection-phase range of more than 360° is obtained from 9.5 GHz to 10.5 GHz. Figure 10 shows amplitude properties of the cross-polarization for the frequency. As we can see from these figure, the cross-polarization level is suppressed to less than about −60 dB for both incidences.

4. Optimized Linear-to-Circular Polarization Conversion

4.1 Linearly-Polarized Wave Properties

We employ the biaxial symmetric shape to realize polarization conversion elements because the elements need to work for the TE and the TM incidences independently.

In order to achieve linear-to-circular polarization conversion, the reflected wave on the reflectarray aperture requires phase difference of 90° between two orthogonal polarizations. Therefore, we employ the biaxial symmetric shape to work for the TE and the TM incidences independently, and also chose the value of ΔP is +90° in the fitness function in (1). It is not suitable for polarization conversion in the case of 90-degree rotational and multiple-axial symmetric shape because the reflection phase properties have the almost same behavior for the TE and the TM incidences. Figure 11 shows polarizer resonant elements designed by GA. Figure 12 shows the characteristics of the reflection phase for the TE and the TM incidences, and phase difference of the reflected waves from 9.0 GHz to 11.0 GHz. We can see that the reflection phase can be changed the range of 360° with 90° phase difference between the reflected waves in the design band. Figure 13 shows the amplitude properties of cross-polarization for both the incidences. The cross-polarization is less than about −60 dB from 9.0 GHz to 11.0 GHz.

4.2 Circularly-Polarized Wave Properties

Figure 14(a) and (b) shows the axial ratio (AR) properties

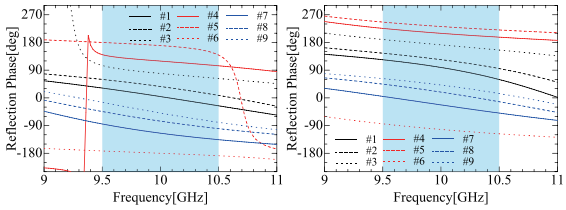

(a) TE incidence. (b) TM incidence.

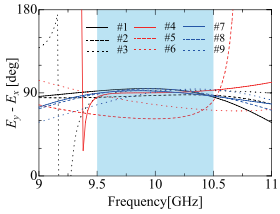

(c) Phase difference.

Fig. 12 Frequency responses of reflection phase for the TE and the TM incidences and phase difference.

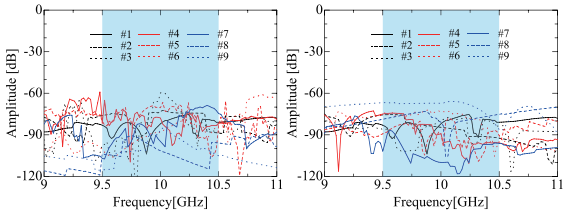

(a) TE incidence. (b) TM incidence.

Fig. 13 Frequency responses of cross-polarization for the TE and the TM incidences.

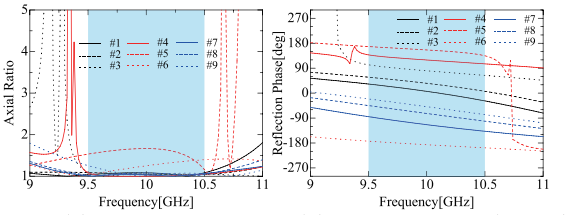

(a) Axial ratio. (b) Reflection phase(LHCP).

Fig. 14 Circularly-polarized wave properties.

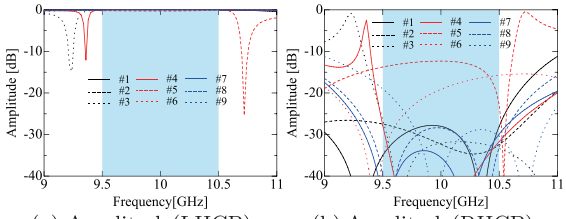

(a) Amplitude(LHCP). (b) Amplitude(RHCP).

Fig. 15 Amplitude properties of circular polarization.

and reflection phase ones of left handed circular polarization (LHCP), respectively. It is clear that AR for all designed elements are less than 2.0, and also LHCP is generated as the co-polarization. Figure 15 show the amplitude of LHCP

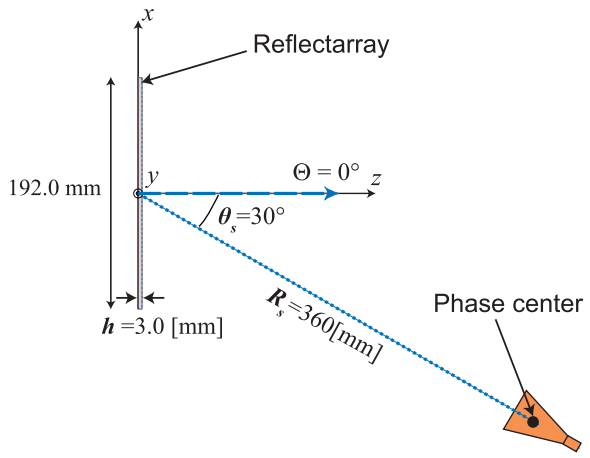

Fig. 16 Parameters of the reflectarray.

and RHCP. It can be seen that the cross-polarization (RHCP) level is less than about −20 dB except for two geometries (# 5 and # 6). It is expected from these results, the proposed elements are useful for constructing a polarizer reflectarray with low cross-polarization by their appropriate arrangement.

4.3 Reflectarray Design

We design a reflectarray in the X-band to confirm effectiveness of the proposed elements. The reflectarray antenna system is shown in Fig. 16. Its dimension is $192 \times 192\,\mathrm{mm}^2$. An offset angle θ_s and the reflected angle Θ are chosen to be 0°. The distance from the phase center of an illuminater (20 dB standard gain horn) to the center of the reflectarray is 360 mm and the edge level is −11 dB. For the offset feed at $\theta_s = 30°$, the angle incident to the element takes the range from 7° to 47°. As a result, we need to consider the phase property of each element on the reflectarray surface corresponding to the incident angle. Figure 17(a) shows the design pattern of the reflecarray. Figure 17(b) shows the aperture phase difference between the TE and the TM waves at the center frequency 10.0 GHz. We can see from this figure that the phase difference is 90°. The fabricated reflectarraay antenna is shown in Fig. 17(c).

4.4 Radiation Patterns

Figure 18 shows the measured radiation patterns of the co- and cross-polarizations for the TE and the TM incidences at 9.0 GHz, 10.0 GHz and 11.0 GHz. It is clear from these figures that the main-beam patterns for both the incident waves agree well with each other. Moreover, the cross-polarization level is almost suppressed less than about −35 dB. Figure 19 shows comparison of the radiation patterns between the calculated and the measured results for the circularly-polarized wave. The calculated far-field patterns of linearly-polarized wave are obtained by using the aperture field method [32]. We can see from these figures that LHCP and RHCP are generated as the co-polarization and cross-polarization, respectively. The main-beam patterns for both the incident

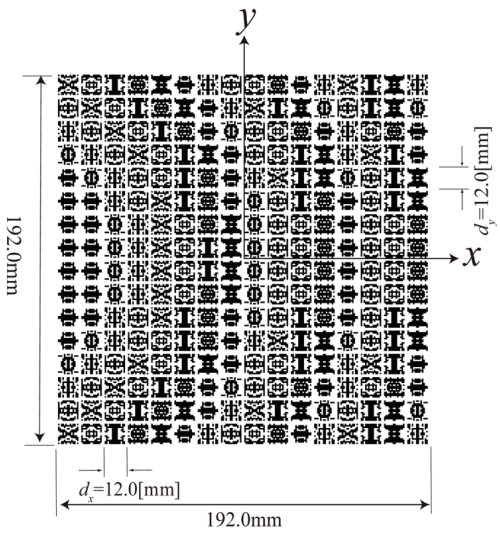

(a) Design pattern.

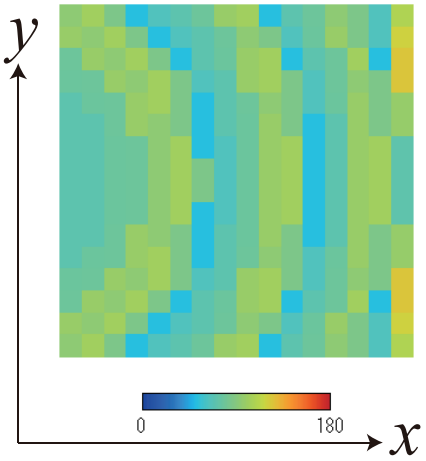

(b) Phase difference.

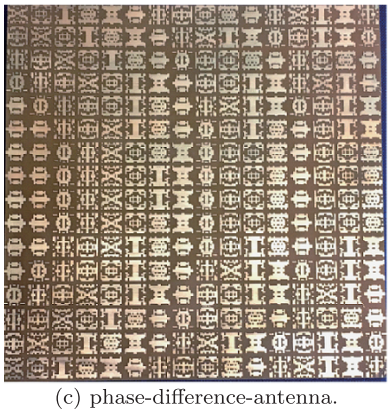

(c) phase-difference-antenna.

Fig. 17 Designed and fabricated reflectarray.

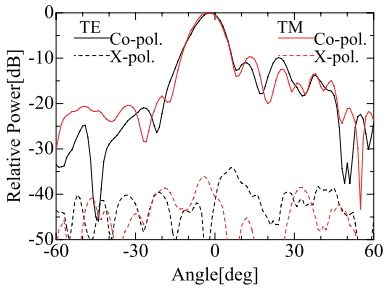

(a) 9.0GHz.

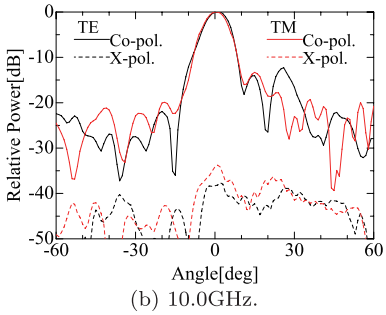

(b) 10.0GHz.

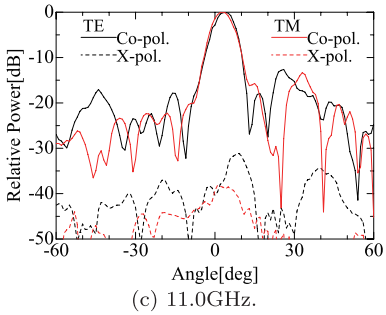

(c) 11.0GHz.

Fig. 18 Radiation patterns of the linearly-polarized wave.

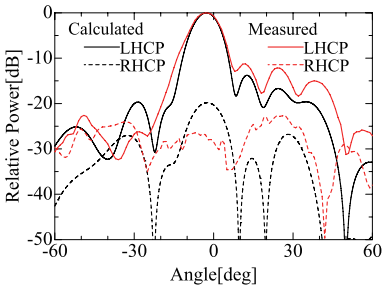

(a) 9.0GHz.

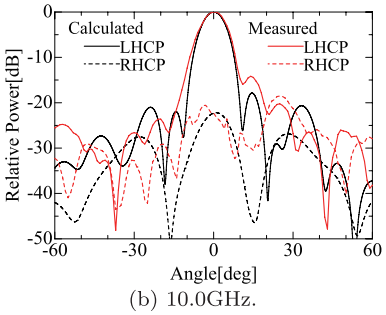

(b) 10.0GHz.

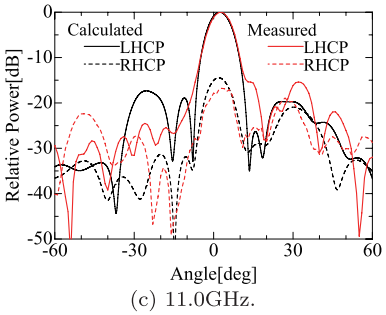

(c) 11.0GHz.

Fig. 19 Radiation patterns of the circularly-polarized wave.

waves agree well with each other. The cross-polarization is less than about −20 dB from 9.0 GHz to 11.0 GHz. Table 1 shows the calculated AR and measured one in design band. It is clear that AR is less than about 1.35 from 9.0 GHz to 11 GHz with fractional bandwidth 20%.

5. Conclusions

We have described how to optimize geometrical structures by using GA for realizing polarization conversion reflectarray. We have presented geometry shapes optimized by using GA for realizing polarization conversion reflectarray. These elements provide almost 90° phase difference with the amount of reflection phase range of 360° over specified frequency. The LHCP is generated as the co-polarization with low cross-polarization (RHCP). To verify the proposed elements, X-band reflectarray is fabricated and is evaluated from radiation property of the circularly-polarized wave through numerical and experimental discussion. As a result, the measured main-beam pattern agrees well with the calculated one

Table 1 Axial ratio of a reflectarray antenna.

Frequency	9.0GHz	9.5 GHz	10 GHz	10.5 GHz	11.0GHz
Calculated AR	1.00	1.18	1.17	1.21	1.06
Measured AR	1.16	1.23	1.21	1.24	1.34

for the circularly polarized waves. The cross polarization level is less than −20 dB in the design band. The calculated and measured axial ratio of the reflectarray are less then about 1.35 from 9.0 GHz to 11.0 GHz with fractional bandwidth 20%, and then usefulness of the proposed elements is verified.

Acknowledgments

This work was supported in part by a Grant-in-aid for Scientific Research (C) (15K06090) from Japan Society for the Promotion of Science.

References

[1] J. Huang and J.A. Encinar, Reflectarray Antennas, Wiley, New Jersey,

2007.
[2] J. Huang, V.A. Feria, and H. Fang, "Improvement of the three-meter Ka-band inflatable reflectarray antenna," IEEE Int. Symp. Antennas Propag., vol.1, pp.122–125, July 2001.
[3] C.R. Dietlein, A.S. Hedden, and D.A. Wikner, "Digital reflectarray considerations for terrestrial millimeter-wave imaging," IEEE Antennas and Wireless Propag. Lett., vol.11, pp.272–275, March 2012.
[4] L. Li, Q. Chen, Q. Yuan, K. Sawaya, T. Maruyama, T. Furuno, and S. Uebayashi, "Frequency selective reflectarray using crossed-dipole elements with square loops for wireless communication applications," IEEE Trans. Antennas Propag., vol.59, no.1, pp.89–98, Jan. 2011.
[5] M. Chaharmir, J. Shaker, and H. Legay,"Broadband design of a single layer large reflectarray using multi cross loop elements," IEEE Trans. Antennas Propag., vol.57, no.10, pp.3363–3366, Oct. 2009.
[6] L. Moustafa, R. Gillard, F. Peris, R. Loison, H. Legayand, and E. Girard, "The Phoenix cell: A new reflectarray cell wtih large bandwidth and rebirth capabilities," IEEE Antennas Wireless Propag. Lett., vol.10, pp.71–74, Jan. 2011.
[7] M. Zhou, S.B. Sorensen, O.S. Kim, E. Jorgensen, P. Meincke, O. Breinbjerg, and G. Toso, "The generalized direct optimization technique for printed reflectarrays," IEEE Trans. Antennas Propag., vol.62, pp.1690–1700, April 2014. vol.62, no.4, pp.1690–1700, 2014.
[8] R. Florencio, J. Encinar, R. Boix, and G. PerezPalomino, "Dual-polarisation reflectarray made of cells with two orthogonal sets of parallel dipoles for bandwidth and cross-polarisation improvement," IET Microw. Antennas Propag., vol.8, no.15, pp.1389–1397, Dec. 2014.
[9] R. Florencio, J. Encinar, R. Boix, V. Losada, and G. Toso, "Reflectarray antennas for dual polarization and broadband telecom satellite applications," IEEE Trans. Antennas Propag., vol.63, no.4, pp.1234–1246, April 2015.
[10] R. Deng, S. Xu, and F. Yang, "Design of Ku/Ka quad-band reflectarray antenna for satellite communications," IEEE Antennas Propag. Symp. Digest, pp.1217–1218, 2016.
[11] H. Hasani, M. Kamyab, and A. Mirkamali, "Low cross-polarization reflectarray antenna," IEEE Trans. Antennas Propag., vol.59, no.5, pp.1752–1756, May 2011.
[12] R. Florencio, J.A. Encinar, R.R. Boix, G. Pérez-Palomino, and G. Toso, "Cross-polar reduction in reflectarray antennas by means of element rotation," Proc. 10th Edition EUCAP, Davos, Switzerland, April 2016.
[13] D.R. Prado, M. Arrebola, M.R. Pino, F. Las-Heras, R. Florencio, R.R. Boix, and J.A. Encinar, "Reflectarray antenna with reduced crosspolar radiation patterns," Proc. 10th Edition EUCAP, Davos, Switzerland, April 2016.
[14] T. Toyoda, D. Higashi, H. Deguchi, and M. Tsuji, "Broadband reflectarray with convex strip elements for dual-polarization use," Proc. International Symposium on Electromagnetic Theory, pp.683–686, 2013.
[15] D. Higashi, H. Deguchi, and M. Tsuji, "Omega-shaped resonant elements for dual-polarization and wideband reflectarray," IEEE Antennas Propag. Symp. Digest, pp.809–810, 2014.
[16] D. Higashi, S. Sasaki, H. Deguchi, and M. Tsuji, "Low cross-polarization reflectarray elements with four axial symmetry for dual-polarization and wideband use," IEEE Antennas Propag. Symp. Digest, pp.2171–2172, 2015.
[17] Y. Aoki, H. Deguchi, and M. Tsuji, "Reflectarray with arbitrarily-shaped conductive elements optimized by genetic algorithm," Proc. International Symposium on IEEE Antennas and Propagation, pp.960–963, 2011.
[18] T. Asada, H. Deguchi, M. Tsuji, and Y. Aoki, "Reflectarray with arbitrary shape elements suppressing their mutual coupling," Proc. International Symposium on Antennas and Propagation (ISAP) 2012, pp.1116–1119, 2012.
[19] T. Asada, S. Matsumoto, H. Deguchi, and M. Tsuji, "Reflectarray with arbitrarily shaped elements having four-axial symmetry," 2014 Asia-Pacific Radio Science Conference Proceedings, pp.1238–1240, 2014.
[20] S. Matsumoto, H. Deguchi, and M. Tsuji, "Shapes of resonant element and their arrangement for better performance of reflectarrays," Proc. APWC, pp.863–866, Torino, Italy, 2015.
[21] T. Moroya, S. Makino, T. Hirota, K. Noguchi, K. Itoh, and K. Ikarshi, "Polarization conversion reflector using metal-plate-loaded meander line," Proc. ISAP, pp.171–172, Dec. 2014.
[22] R. Orr, G. Goussetis, V. Fusco, and E. Saenz, "Linear-to-circular polarization reflector with transmission band," IEEE Trans. Antennas Propag., vol.63, no.5, pp.1949–1956, May 2015.
[23] G. Wu, S. Qu, S. Yang, and C. Chan, "Broadband, single-layer dual circularly polarized reflectarrays with linearly polarized feed," IEEE Trans. Antennas Propag., vol.64, no.10, pp.4235–4241, Oct. 2016.
[24] R. Shibayama, H. Deguchi, and M. Tsuji, "Flat thin polarizer-lens based on multiple resonance behavior," IEEE Antennas Propag. Symp. Digest, pp.1–4, 2010.
[25] D. Higashi, S. Sasaki, H. Deguchi, and M. Tsuji, "Polarizer reflectarray using resonant behavior of orthogonal elements for wideband use," Proc. International Symposium on IEEE Antennas and Propagation, pp.1207–1208, 2016.
[26] S. Matsumoto, H. Yamada, H. Deguchi, and M. Tsuji, "Reflectarray with aribitrarily shaped elements for linear-to-circular polarization," Proc. ISAP, pp.650–651, Dec. 2016.
[27] T.K. Wu, Frequency Selective Surface and Grid Array, New York, Wiley, 1995.
[28] R. Mittra, C.H. Chan, and T. Cwik, "Techniques for analyzing frequency selective surfaces-A review," Proc. IEEE, vol.76, no.12, pp.1593–1615, Dec. 1988.
[29] T. Asada, H. Deguchi, M. Tsuji, and Y. Aoki, "Optimization of arbitrary elements suppressing their mutual coupling in reflectarray," IEICE Technical Report, EMT-12-159, Nov. 2012.
[30] T. Asada, H. Deguchi, and M. Tsuji, "Optimization of arbitrarily shaped elements suppressing cross-polarization component in reflectarray," IEICE Technical Report, EMT-13-148, Nov. 2013.
[31] Y. Rahmat, "An efficient computational method for characterizing the effects of random surface errors on the average power pattern of reflectors," IEEE Trans. Antennas Propag., vol.AP-31, no.1, pp.92–98, Jan. 1983.
[32] S. Silver, Microwave Antenna Theory and Design, IET, 1949.

Hiroyuki Deguchi was born in Osaka, Japan, on Aug. 24, 1962. He received the B.E., M.E., and D.E. degrees from Doshisha University, Kyoto, Japan, in 1986, 1988, and 1999, respectively. From 1988 to 2000, he was with the Mitsubishi Electric Corporation. Since 2000, he has been with Doshisha University, where he is currently a Professor. His current research activities are concerned with microwave and millimeter-wave aperture antennas and antenna measurements. Prof. Deguchi is a member of the Institute of Electronics, Information and Communication Engineers (IEICE), Japan, and the Institute of Electrical Engineers (IEE), Japan. He was the recipient of the 1992 IEICE Young Engineer Award.

Daichi Higashi was born in Okayama, Japan, on Feb. 25, 1991. He received the B.E., and M.E. degrees from Doshisha University, Kyoto, Japan, in 2013 and 2015, respectively. Currently, he is a student of the Graduate School of Electric Engineering, Doshisha University. His current research activities are concerned with the analysis and design of the reflectarray antennas and the metasurfaces. Mr. Higashi is a Member of the Institute of Electronics, Information and Communication Engineers (IEICE), Japan.

Hiroki Yamada was born in Shiga, Japan, on Nov. 20, 1993. He received the B.E. degrees from Doshisha University, Kyoto, Japan, in 2016, respectively. Currently, he is a student of the Graduate School of Electric Engineering, Doshisha University. His current research activities are concerned with the analysis and design of the reflectarray antennas.

Shogo Matsumoto was born in Hyogo, Japan, on June 8, 1991. He received the B.E., and M.E. degrees from Doshisha University, Kyoto, Japan, in 2014 and 2016, respectively. Since 2016, he joined Honda Motor Co., Ltd. Between 2014 and 2016, he had been engaged in research and developments of analysis and design of the reflectarray antennas.

Mikio Tsuji was born in Kyoto, Japan, on Sept. 10, 1953. He received the B.E., M.E., and D.E. degrees from Doshisha University, Kyoto, Japan, in 1976, 1978, and 1985, respectively. Since 1981, he has been with Doshisha University, where he is now a Professor. His present research activities are concerned with microwave and millimeter-wave guiding structures and devices and scattering problems of electromagnetic waves. Prof. Tsuji is a member of the Institute of Electronics, Information and Communication Engineers (IEICE) of Japan and the Institute of Electrical Engineers (IEE) of Japan.